
This is an electronic reprint of the original article.
This reprint may differ from the original in pagination and typographic detail.

Belt, Tiina; Keplinger, Tobias; Hänninen, Tuomas; Rautkari, Lauri

Cellular level distributions of Scots pine heartwood and knot heartwood extractives revealed by Raman spectroscopy imaging

Published in:
Industrial Crops and Products

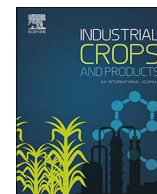
DOI:
[10.1016/j.indcrop.2017.06.056](https://doi.org/10.1016/j.indcrop.2017.06.056)

Published: 01/12/2017

Document Version
Publisher's PDF, also known as Version of record

Published under the following license:
CC BY

Please cite the original version:
Belt, T., Keplinger, T., Hänninen, T., & Rautkari, L. (2017). Cellular level distributions of Scots pine heartwood and knot heartwood extractives revealed by Raman spectroscopy imaging. *Industrial Crops and Products*, 108, 327-335. <https://doi.org/10.1016/j.indcrop.2017.06.056>



Cellular level distributions of Scots pine heartwood and knot heartwood extractives revealed by Raman spectroscopy imaging



Tiina Belt^{a,1,*}, Tobias Keplinger^{b,c,1}, Tuomas Hänninen^a, Lauri Rautkari^a

^a Aalto University, School of Chemical Engineering, Department of Bioproducts and Biosystems, P.O. Box 16300, 00076 Aalto, Finland

^b Wood Materials Science, Institute for Building Materials, ETH Zurich, Stefano-Franscini-Platz 3, 8093 Zurich, Switzerland

^c Applied Wood Materials, EMPA Swiss Federal Laboratories for Materials Science and Technology, Ueberlandstrasse 129, 8600 Dübendorf, Switzerland

ARTICLE INFO

Keywords:

Extractives
Heartwood
Imaging
Pinosylvin
Raman spectroscopy
Scots pine

ABSTRACT

Wood extractives are biologically active secondary metabolites that help protect wood and wood products from decay and other forms of biological attack. Despite the influence of distribution on their ability to protect wood, very few studies have investigated the distributions of extractives on a cellular level. In this paper, the distributions of extractives were studied in Scots pine (*Pinus sylvestris* L.) heartwood (HW) and knot heartwood by confocal Raman spectroscopy imaging. Pinosylvins, the antifungal phenolic extractives of pine, were found to be present in the cell walls, middle lamella, and lumina of tracheids. Their distribution suggested the existence of two different mechanisms of deposition and revealed similarities to the distribution of lignin. The potential binding of pinosylvins to lignin and their relatively low concentration in HW cell walls could explain why Scots pine HW is, on average, only moderately resistant to decay. Resin acids, the most abundant group of extractives in pine, were detected only within the lumina of tracheids and ray cells, where they may contribute to the reduced permeability of HW. The extractives distributions presented here help us understand the properties of HW and provide a deeper understanding of the origins of natural durability, which is of value in the current efforts to develop more environmentally friendly means of wood protection.

1. Introduction

Wood is a complex natural composite consisting primarily of cellulose, hemicelluloses, and lignin. In addition to these structural polymers, wood also contains secondary metabolites called extractives, which occur primarily in the heartwood (HW) and knot heartwood (KHW) of trees. Although they are often low in abundance compared to the structural components, the extractives have a significant effect on the properties of wood, most notably its resistance to decay and other forms of biological attack (Hillis, 1987; Taylor et al., 2002). Due to the economic and biological significance of decay resistance, the chemical composition, properties, and formation of extractives have been extensively studied (Hillis, 1987; Taylor et al., 2002; Kampe and Magel, 2013).

In Scots pine (*Pinus sylvestris* L.), a commercially important species in northern Europe, the HW and KHW extractives consist mainly of the phenolic pinosylvins and the hydrophobic resin acids and fatty acids (Piispanen and Saranpää, 2002; Willför et al., 2003; Ekeberg et al., 2006; Hovelstad et al., 2006; Fang et al., 2013). The knots of Scots pine are often particularly rich in extractives and contain lignans in addition

to the HW extractives (Willför et al., 2003, 2004; Hovelstad et al., 2006; Fang et al., 2013). Pinosylvins and resin acids have both been linked to the decay resistance of pine HW (Harju et al., 2002; Venäläinen et al., 2004; Leinonen et al., 2008), and attempts have even been made to utilize these compounds as environmentally friendly wood protection agents (Celimene et al., 1999; Lu et al., 2016).

Despite extensive characterization of composition and properties, very little is known about the deposition pathways and cellular level distributions of Scots pine extractives. Knowledge of the incorporation and formation of extractives is necessary to gain a full understanding of HW formation, but the distribution of extractives also has a significant effect on their ability to modify wood properties (Taylor et al., 2002). The distribution of pinosylvins is of particular interest, due to the disparity that exists between the high antifungal activity of pinosylvins and the moderate decay resistance of the HW of various pine species (Hart and Shrimpton, 1979). The decay resistance and pinosylvins content Scots pine HW are highly variable (Bergström et al., 1999; Fries et al., 2000; Harju and Venäläinen, 2002; Venäläinen et al., 2004), and the average resistance of its HW is typically classified as only moderate or slight (Jebrane et al., 2014; Plaschki et al., 2014). It has been

* Corresponding author.

E-mail address: tiina.belt@aalto.fi (T. Belt).

¹ These authors contributed equally.

suggested that the inability of pinosylvins to confer significant decay resistance to wood may be due to their distribution or binding to lignin (Hart and Shrimpton, 1979).

In other wood species, a small number of studies have been performed to investigate the distribution of HW extractives (Kuo and Arganbright, 1980; Streit and Fengel, 1994; Nagasaki et al., 2002; Zhang et al., 2004; Imai et al., 2005). However, most of these studies have used non-specific staining rather than methods that allow for the visualization of defined chemical components. One of the most promising methods for distribution mapping of specific chemical components is confocal Raman spectroscopy imaging. Raman imaging yields spatially resolved chemical information without staining or labeling and has previously been used to investigate the distributions of wood cell wall polymers (Agarwal, 2006; Gierlinger and Schwanninger, 2006; Hänninen et al., 2011; Ji et al., 2013; Gierlinger, 2014; Zhou et al., 2014) and extraneous compounds inserted into the cell walls (Ermeýdan et al., 2012; Keplinger et al., 2015; Merk et al., 2015).

In this study, Raman spectroscopy imaging was applied to the study of native wood extractives. Extractives distributions were investigated in Scots pine HW and KHW, with a focus on pinosylvins. The study aimed to provide additional insight into HW formation and increase our understanding of the properties and behavior of HW, particularly in terms of natural durability. A deeper understanding of the origins of natural durability will help in the current efforts to develop more environmentally friendly means of wood protection. New insights into the distributions of different types of extractives also provide valuable information on the inherent transportation pathways within wood, which is of great interest in the field of wood modification and functionalization.

2. Materials and methods

2.1. Chemicals

Pinosylvins, pinosylvins monomethyl ether, abietic acid, isopimaric acid, linoleic acid, and oleic acid were purchased from Sigma Aldrich and were used as received.

2.2. Wood material

Two green Scots pine logs were obtained from a sawmill in southern Finland and stored frozen until use. The sapwood and heartwood

samples were both prepared from one log, which was mature (70 annual rings) and free of defects. A disc approx. 50 mm thick was sawn from the log, and a strip approx. 80 mm wide was sawn through the center of the disc. Sapwood (SW), outer heartwood (OWH), and middle heartwood (MHW) sections, each containing approx. 5 annual rings, were prepared from the strip as shown in Fig. 1a. HW was visually identified by its lighter color due to its lower moisture content. Each section was cut in half across the grain: one half was cut with a razor blade into sticks with a 5 × 5 mm cross-section, while the other half was cut into small pieces and ground in a Wiley mill.

Knot samples were prepared from the other log (27 annual rings) which was rich in knots. A thick disc containing a whorl of branches was sawn from the log, and the disc was split into four sections. Live knots were removed from each section (Fig. 1b,c) and trimmed until only knot heartwood (KHW) remained (Fig. 1d). One half of the knot material was cut into sticks as described above, while the other half was again ground in a Wiley mill.

After preparation, the wood sticks and powders were air-dried. A small portion of each air-dried powder was also dried at 105 °C to determine the residual moisture content of the powders. Each powder was then Soxhlet extracted with acetone (6 h), and the composition of each extract was analyzed by GC–MS. Some of the sticks were also extracted with acetone, after which the extracted and unextracted sticks were used for Raman spectroscopy imaging.

2.3. GC–MS analysis

A small aliquot of each extract and the internal standard (heneicosanoic acid) was added to a vial and the solvent evaporated under vacuum. The extracts were redissolved in 700 µL of pyridine and trimethylsilylated at 70 °C for 20 min after addition of 300 µL N,O-bis(trimethylsilyl)trifluoroacetamide with 5% chlorotrimethylsilane. The compounds present in the extracts were identified and quantified using a Thermo Scientific ISQ series single quadrupole mass spectrometer, coupled with a Trace 1300 gas chromatograph. The column used was TR-5MS (30 m × 0.25 mm i.d., 0.25 µm film thickness), and the oven temperature program was set to 2 min at 100 °C, 15 °C/min to 280 °C, and 15 min at 280 °C. Helium was used as the carrier gas (1 mL/min), and the mass spectra were recorded in the 50–700 (*m/z*) range at an ionization energy of 70 eV. Each extract was analyzed in duplicate.

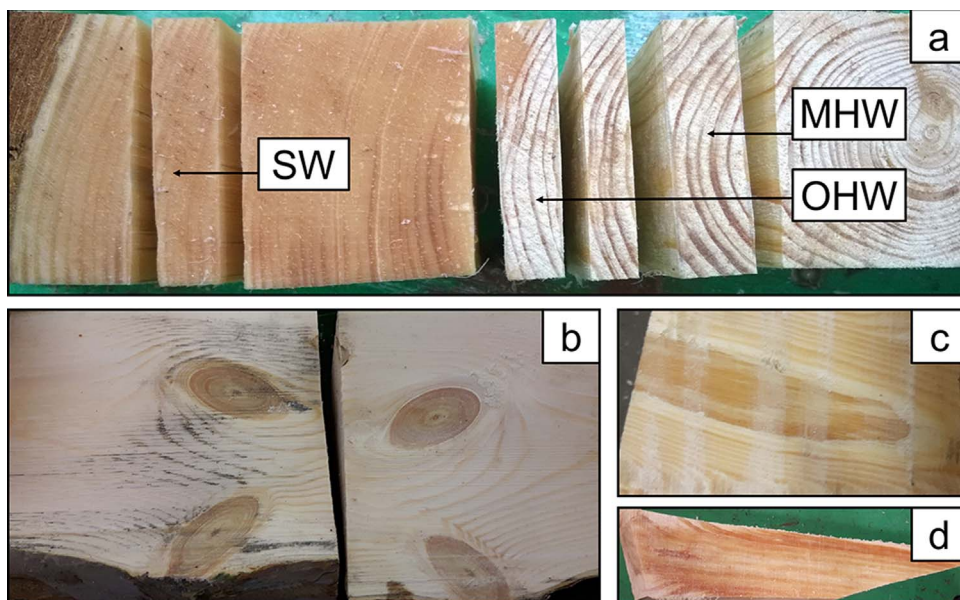


Fig. 1. Sampling of sapwood (SW), outer heartwood (OWH), middle heartwood (MHW) and knot heartwood (KHW). The position of SW, OWH, and MHW in the cross section of the disc (a), and the processing of knot samples, showing knots in the disc sections (b), a knot removed from one section (c), and a final trimmed KHW sample (d).

2.4. Raman spectroscopy

2.4.1. Raman sample preparation

The wood samples were prepared for Raman imaging according to Gierlinger et al. (2012). Briefly, 8 μm thick cross sections of the various wood samples were prepared with a rotary microtome (RM 2255, Leica). The cross sections were put on glass microscope slides, a couple of drops of deionized water were added, and glass cover slips were placed on top of the samples. Cross-sections of each sample type were prepared from three different sticks.

2.4.2. Confocal raman spectroscopy measurements and data analysis

Confocal Raman imaging was performed on latewood portions of the sample cross-sections, and each cross-section was separately analyzed at least three times. The measurements were performed using a Renishaw inVia Raman microscope equipped with a 532 nm laser, an oil immersion objective (Nikon, 100 \times , NA = 1.4), and a 1800 L/mm grating. A step size of 300 nm was chosen in the StreamlineHR mode. The size of a typical measurement area was 30–100 \times 30–100 μm . After the measurement, a cosmic ray removal filter was applied and the spectra were baseline corrected in the measurement software Wire 4.1. For analysis the spectra were exported to Cytospec (v.2.00.01), a commercially available Matlab based software, and plotted in Origin Pro 8.1.

2.4.3. Raman spectroscopy of reference substances

Reference substances were put on microscope slides and measured with a 50 \times air objective (Nikon, NA = 0.9) and a 532 nm laser.

3. Results and discussion

3.1. Extractives composition of wood materials

Table 1 shows the gravimetric yields of extractives obtained from the wood materials, as well as the yields of pinosylvins, resin acids, and fatty acids. The characterization was limited to these main compound groups, as it was done to support the following Raman spectroscopic analysis. For more information on the extractives composition of Scots pine, the reader is referred to specialized literature (Piispanen and Saranpää, 2002; Willför et al., 2003, 2004; Ekeberg et al., 2006; Hovelstad et al., 2006; Arshadi et al., 2013; Fang et al., 2013).

SW contained the lowest amount of extractable components and no detectable pinosylvins. The SW extract contained only minor amounts of resin acids, fatty acids or other monomeric extractives, suggesting that the extract consisted of mostly higher molecular weight material such as triglycerides, which are known to occur in significant quantities in sapwood (Piispanen and Saranpää, 2002; Willför et al., 2003).

The two HW samples (MHW and OHW) were richer in extractives, with resin acids as the dominant extractives component. MHW, in particular, contained very large amounts of resin acids. Pinosylvins (PS) and pinosylvins monomethyl ether (PSM) were also present in the HW samples, and the analysis indicated that in this case their concentrations were higher in MHW than OHW. This is in contrast to previous studies (Bergström et al., 1999; Bergström, 2003; Ekeberg et al., 2006), which demonstrated that pinosylvins content reached its maximum in the

transition zone and then declined in mature HW. However, these studies also demonstrated that there was significant between-tree variation in the lateral location of the concentration maximum and in the extent of decline after the maximum had been reached (Bergström et al., 1999; Bergström, 2003). As no attempts were made in this study to locate the concentration maximum of pinosylvins, it is likely that the OHW sample consisted mostly of early HW where the concentration maximum has not yet been reached.

The knot sample contained very large amounts of extractives, 42% of the dry weight of the knots. Resin acids were the dominant extractives component, but pinosylvins were also present at very high concentrations, accounting for 6.6% of the weight of the knots. Extractives contents of equal magnitude have been previously reported in Scots pine knots (Willför et al., 2003; Fang et al., 2013; Karpunen et al., 2007). The concentrations of free fatty acids and other extractives were very low compared to those of resin acids and pinosylvins.

3.2. Raman spectra of extractives reference compounds

Raman spectroscopy probes all wood constituents at the same time, resulting in complex spectra characterized by many overlapping bands arising from the various structural and non-structural cell wall components. Thus, to be able to distinguish the spectral contributions of the extractives from those of the cell wall polymers, reference spectra were measured for the two pinosylvins (PS and PSM) and two fatty acid and resin acid representatives (Fig. 2; see Table 2 for band assignments). Linoleic acid and oleic acid represent the two most common fatty acids found in pine, and abietic and isopimaric acid represent the abietane- and pimarane- type resin acids, respectively. The discussion of the spectra is limited to the spectral regions used later for the analysis of the wood spectra. More detailed analyses of the spectra of the reference substances can be found elsewhere (Billes et al., 2002; Czamara et al., 2015; Talian et al., 2010).

Apart from slight changes in band positions, the measured spectrum of PS was similar to that published by Holmgren et al. (1999). The spectrum featured characteristic bands at 1634, 1597, and 994 cm^{-1} , attributed to olefinic C=C stretching, aromatic ring stretching, and vibration of the 1,3,5-substituted aromatic ring, respectively. Nevertheless, small yet significant differences could be seen in the spectral region attributed to the substituted aromatic ring stretching. The band at 994 cm^{-1} has been described as a single peak (Holmgren et al., 1999), but the spectrum in Fig. 2 clearly shows that it was accompanied by a shoulder at 998 cm^{-1} , which has not been previously reported. The spectrum of PSM was similar to that of PS, distinguishable by a shift of the band at 1634 cm^{-1} to 1638 cm^{-1} and the occurrence of an additional band at 1608 cm^{-1} . Interestingly, the shoulder visible at 998 cm^{-1} in the spectrum of PS was not detected in the PSM spectrum.

The spectra of linoleic and oleic acid were similar to one another, producing characteristic bands at 1658 and 1654 cm^{-1} , respectively, attributed to the stretching vibration of the C=C double bond. The spectrum of abietic acid was characterized by one intense C=C stretching band at 1649 cm^{-1} , whereas isopimaric acid revealed C=C stretching bands at 1666 and 1638 cm^{-1} , and a number of C–H and C–C vibrations at wavelengths below 1500 cm^{-1} .

3.3. Raman spectroscopy imaging of wood samples

In confocal Raman spectroscopy imaging, a large number of Raman spectra are collected from the sample to build a map in which every pixel consists of an individual spectrum. The unextracted and extracted SW, OHW, MHW, and KHW samples were mapped in this fashion, and false color images were generated by integration over 1550–1700 cm^{-1} to visualize the cell structure (Fig. 3a–h). Average spectra were then extracted from the cell wall (CW) and cell corner (CC) regions (Fig. 3i,j). The spectra showed typical features of wood, revealing spectral contributions from cellulose and lignin within the CW and

Table 1

Extractives composition of sapwood (SW), outer heartwood (OHW), middle heartwood (MHW), and knot heartwood (KHW) as determined by GC–MS (mg per g O.D. wood).

	SW	OHW	MHW	KHW
Gravimetric yield	28.7	74.6	228.9	420.0
Pinosylvins	–	7.3	12.3	66.1
Resin acids	1.0	42.0	178.6	285.7
Fatty acids	0.8	3.7	3.7	2.5
Other	2.7	1.5	0.9	14.8

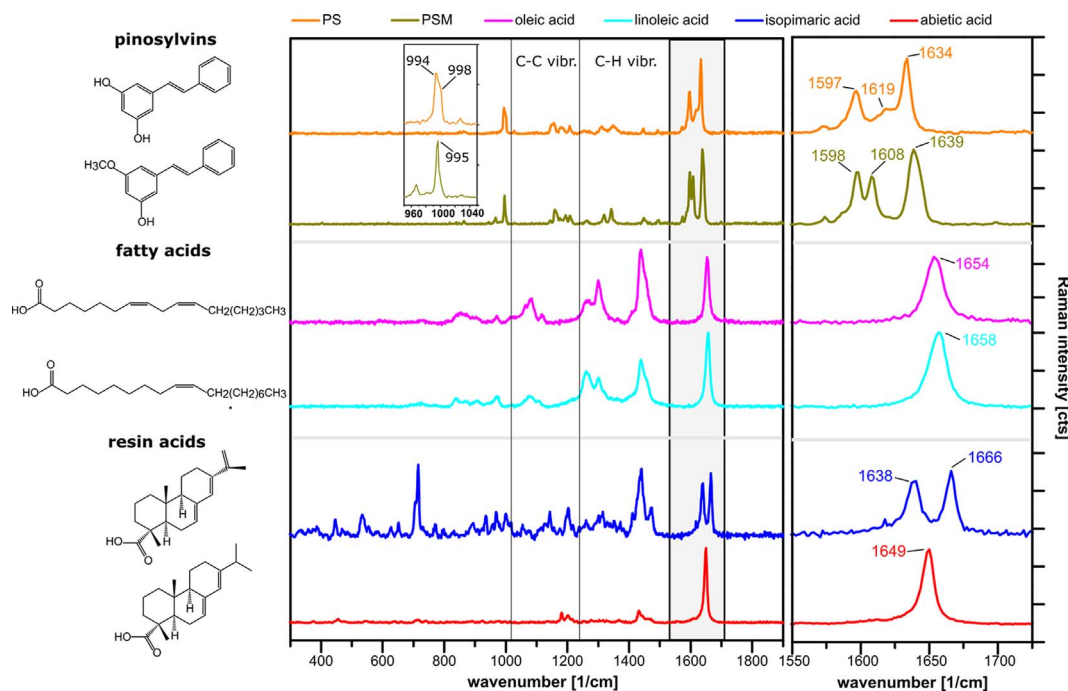


Fig. 2. Raman spectra of extractives reference compounds. PS, pinosylvin; PSM, pinosylvin monomethyl ether.

mostly those from lignin in the CC. Characteristic peaks of cellulose include, for example, the C–C–C ring vibration at 380 cm^{-1} and the C–O–C glycosidic vibration at 1098 cm^{-1} (Edwards et al., 1994). The most prominent band of lignin, 1600 cm^{-1} , is attributed to symmetric aryl ring stretching, while the band at 1657 cm^{-1} is due to the ring conjugated C=C stretching of coniferyl alcohol and the C=O stretching of coniferaldehyde (Agarwal and Ralph, 2008).

The average CW and CC spectra of unextracted HW and KHW showed two bands not present within the spectra of SW, 1634 and 995 cm^{-1} . These bands correspond to the C=C stretching vibrations and the substituted aromatic ring vibrations of pinosylvins (Fig. 2), suggesting the presence of pinosylvins in the CW and the CC. Previous workers have also detected these two bands in Scots pine HW and knots and attributed them to the pinosylvins (Holmgren et al., 1999; Nuopponen et al., 2004b). However, while the 1634 cm^{-1} band is characteristic of pinosylvins and has been used in previous investigations to measure their concentration in wood (Bergström et al., 1999; Bergström, 2003), it cannot be assumed to be solely due to pinosylvins. Isopimaric acid (Fig. 2) and other pimarane-type resin acids also produce bands in this spectral region (Nuopponen et al., 2004a), and other extractives may do the same. Hence, in this study the band at 995 cm^{-1} was chosen as the marker band for pinosylvins. The band arises from a structure unique to the pinosylvins, although it cannot be used to distinguish PS and PSM.

The intensity of the 995 cm^{-1} band varied from sample to sample, indicating differences in the concentration of the pinosylvins (Fig. 3). The band was nearly absent in SW samples and gradually increased in intensity from OHW to MHW to KHW, in agreement with the pinosylvin concentrations determined by GC–MS (Table 1). The intensity of the band was drastically reduced by extraction, providing further support that it is indeed derived from extractable compounds. However, extraction did not completely eliminate the pinosylvins signal, suggesting that not all pinosylvins can be removed by simple Soxhlet extraction.

Interestingly, no bands corresponding to the C=C stretching vibrations of abietane-type resin acids or fatty acids were detected in any of the CW and CC spectra, despite the significant resin acid content of the HW and KHW samples (Table 1). Two possible explanations exist for this: 1, resin acids (and fatty acids) are not located in the CW and CC

of tracheids, or 2, resin acids cannot be detected due to their relatively low concentration and lack of resonance effects. The Raman signals of conjugated molecules such as pinosylvins are resonance enhanced at certain laser wavelengths and can be detected within complex spectra even at low concentrations. However, the second explanation seems unlikely, considering that substantial amounts of resin acids were present in samples such as KHW (Table 1). Raman spectroscopy has also been shown to be quite sensitive to incorporated molecules (Ermejdán et al., 2012; Keplinger et al., 2015; Merk et al., 2015), suggesting that resin acids are actually absent in the CW and CC.

Table 2
Band assignments for extractives reference compounds.

Substance	Band (cm^{-1})	Vibration
PS ^a	1634, 1619	C=C stretching
	1597	symmetric aromatic ring stretching
	1349, 1310	CH ₂ /CH ₃ deformation
	1156, 1179, 1185	C–C skeletal mode
	994, 998	1,3,5-substituted aromatic ring
PSM ^b	1639, 1608	C=C stretching
	1598	symmetric aromatic ring stretching
	1342, 1319	CH ₂ /CH ₃ deformation
	1159, 1176, 1194	C–C skeletal mode
	995	1,3,5-substituted aromatic ring
Oleic acid	1654	C=C stretching
	1439, 1301, 1261	CH ₂ /CH ₃ deformation
	909, 971, 1076	C–C skeletal mode
Linoleic acid	1658	C=C stretching
	1439, 1301, 1261	CH ₂ /CH ₃ deformation
	909, 971, 1076	C–C skeletal mode
Isopimaric acid	1666, 1638	C=C stretching
	1410, 1441, 1472	CH ₂ /CH ₃ deformation
	1144, 1202	C–C skeletal mode
Abietic acid	1649	C=C stretching
	1444, 1432	CH ₂ /CH ₃ deformation
	1181, 1202	C–C skeletal mode

^a Pinosylvin.

^b Pinosylvin monomethyl ether.

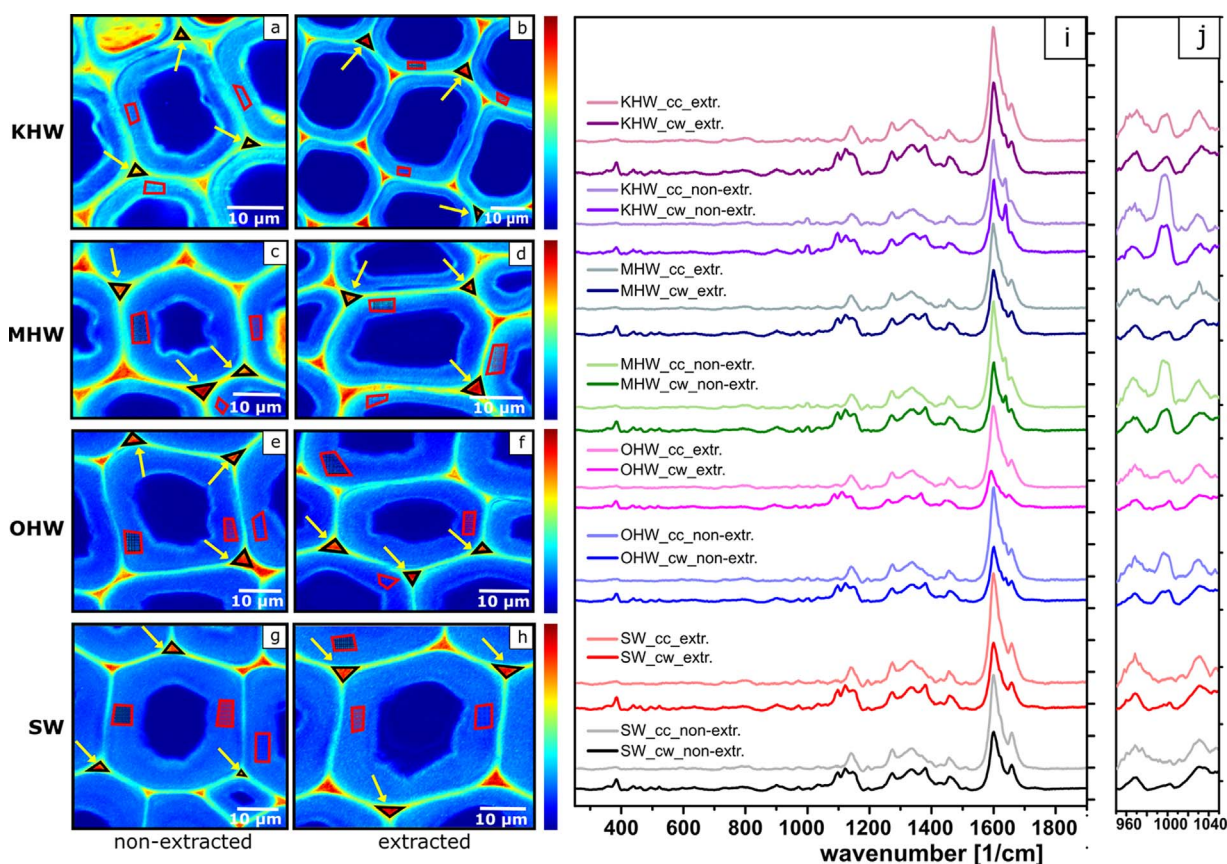


Fig. 3. Average cell wall (CW) and cell corner (CC) Raman spectra of unextracted and extracted sapwood (SW), outer heartwood (OHW), middle heartwood (MHW) and knot heartwood (KHW). Cell visualization (by integration over $1550\text{--}1770\text{ cm}^{-1}$) (a–h), and average CW and CC spectra (i and j), obtained from regions indicated on the cell visualization images. (For interpretation of the references to colour in this figure legend, the reader is referred to the web version of this article.)

The distributions of cellulose ($1065\text{--}1102\text{ cm}^{-1}$, Fig. 4a,e,i,m,q,u), lignin ($1104\text{--}1173\text{ cm}^{-1}$, Fig. 4b,f,j,n,r,v), and pinosylvins ($985\text{--}1009\text{ cm}^{-1}$, Fig. 4d,h,l,p,t,x) were investigated in more detail by integration of specific marker bands. Integrations revealed that cellulose had the highest intensity in the CW and lignin in the CC and compound middle lamella (CML), which is in good agreement with previously published results (Agarwal, 2006; Gierlinger and Schwanninger, 2006; Hänninen et al., 2011; Gierlinger, 2014). The high cellulose intensity visible in the S1 layer is due to the increased microfibril angle, to which the selected cellulose band is sensitive (Gierlinger et al., 2010). In this investigation, the band at $1104\text{--}1173\text{ cm}^{-1}$ was used as a marker for lignin rather than, for example, $1550\text{--}1640\text{ cm}^{-1}$ due to interference from extractives. The combined distribution of lignin and extractives is shown in Fig. 4(c,g,k,o,s,w).

Integration of the pinosylvins marker band clearly highlighted the differences in pinosylvins concentration between the samples. The intensity of the pinosylvins marker band was relatively low within OHW and increased in MHW and KHW, which is in agreement with the pinosylvins concentrations measured by GC–MS (Table 1). Despite concentration differences, all of the unextracted samples showed a similar distribution pattern: the amount of pinosylvins increases from CW to CML to CC. The distribution of pinosylvins therefore appears to follow that of lignin, suggesting that there may be an interaction between the two components. Binding of pinosylvins to lignin has been previously hypothesized (Hart and Shrimpton, 1979; Mohammed-Ziegler et al., 2004), and in other wood species phenolic extractives have been detected in association with lignin (Helm et al., 1997). Together with their relatively low cell wall concentration, the potential binding of pinosylvins to lignin could serve to reduce the decay resistance of Scots pine

HW and offset the high antifungal activity of isolated pinosylvins. The binding of pinosylvins might also explain their partial resistance to solvent extraction.

The relatively high concentration of pinosylvins in the CC/CML also suggests that their deposition during HW formation may involve movement through the CML. Previous research has indicated that some HW extractives are released from parenchyma cells into intercellular spaces, from where they diffuse into the CML and slowly begin to impregnate the cell walls (Streit and Fengel, 1994; Zhang et al., 2004). Coloring matter of unspecified composition has previously been observed in the CC/CML of Scots pine (Fengel, 1970), and the results presented here suggest that it may have been pinosylvins.

In addition to the CC, CML and CW, pinosylvins were also detected within tracheid lumina. Two different types of deposits were present: some tracheids appeared to be entirely filled with pinosylvins-rich material, while others only contained small deposits or a thin lining on the lumen wall.

3.4. Analysis of extractives deposits

The extractives deposits of HW and KHW samples were analyzed in more detail by light microscopy and Raman imaging. A light microscopy image of MHW (Fig. 5a) shows that both types of deposits were present within the sample. The presence of deposits was also confirmed by wide area Raman mapping (Fig. 5b), but a more detailed analysis of the spectra (Fig. 5c,d) revealed that there were significant differences in the chemical composition of the small deposits and the lumen-filling material. The small deposits were rich in pinosylvins, as evidenced by strong pinosylvins-derived bands at 995 , 1597 , 1608 , and 1634 cm^{-1} (Fig. 2) and the absence of other prominent bands. The deposits most

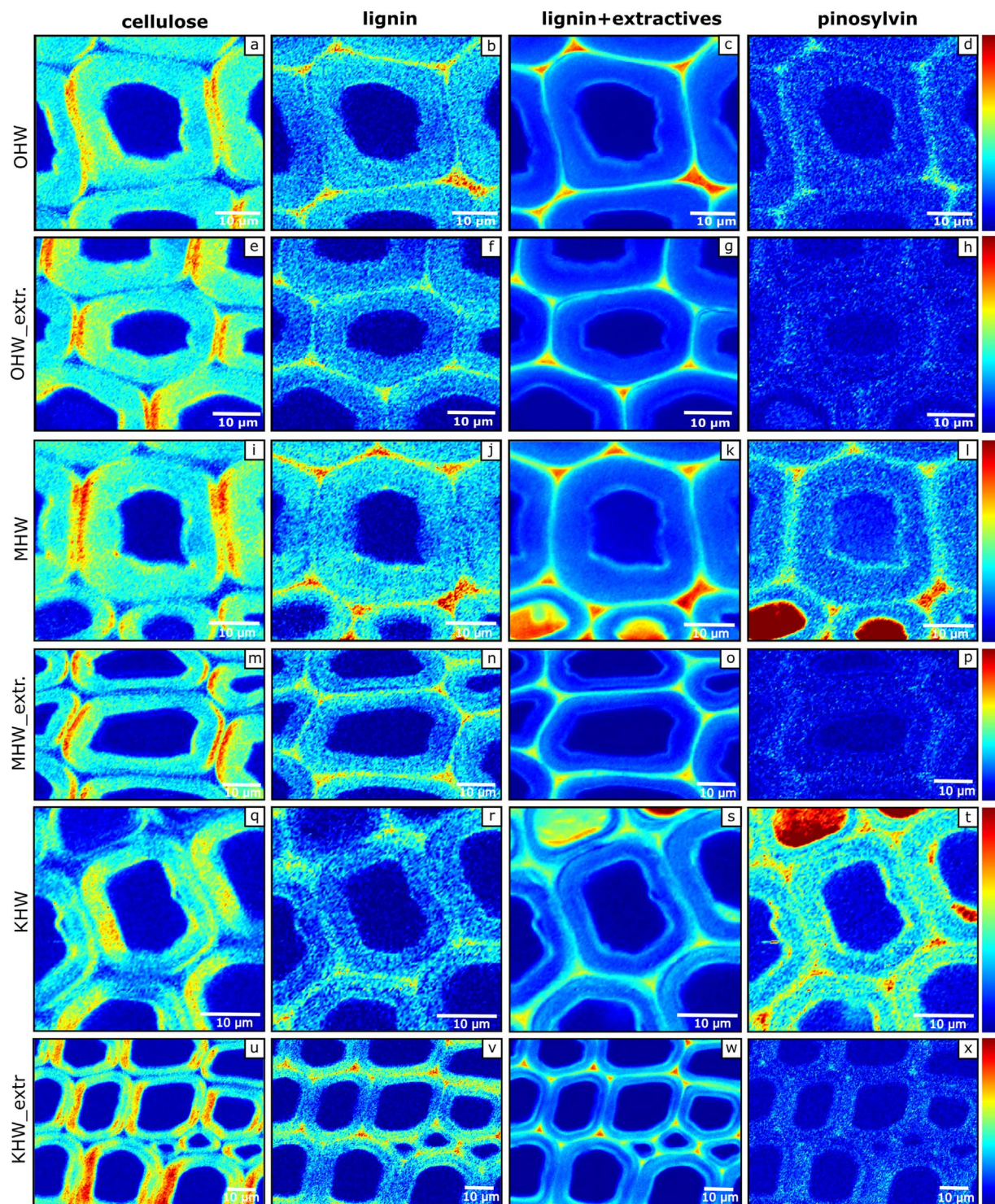


Fig. 4. Raman imaging of unextracted and extracted outer heartwood (OHW), middle heartwood (MHW), and knot heartwood (KHW), showing the distributions of cellulose (integration over $1065\text{--}1102\text{ cm}^{-1}$) (a,e,i,m,q,u), lignin ($1104\text{--}1173\text{ cm}^{-1}$) (b,f,j,n,r,v), lignin + extractives ($1538\text{--}1690\text{ cm}^{-1}$) (c,g,k,o,s,w), and pinosylvin ($985\text{--}1009\text{ cm}^{-1}$) (d,h,l,p,t,x). (For interpretation of the references to colour in this figure legend, the reader is referred to the web version of this article.)

likely arose from the movement of pinosylvins from cell to cell via pit connections, as has been observed with the HW extractives of other wood species (Kuo and Arganbright, 1980; Streit and Fengel, 1994; Nagasaki et al., 2002; Zhang et al., 2004). The movement of unspecified coloring matter from cell to cell via pits has also been previously recorded in Scots pine (Fengel, 1970).

In contrast to the small deposits, the lumen-filling material within

MHW and KHW samples contained significantly lower amounts of pinosylvins, as evidenced by the reduced relative intensity of the pinosylvins-derived bands. Instead, the spectra were characterized by an intense band at 1649 cm^{-1} , which corresponds to abietic acid (Fig. 2) and other abietane-type resin acids (Nuopponen et al., 2004a). A second prominent band was observed at 1612 cm^{-1} , attributed to the symmetric aromatic ring stretch of dehydroabietic acid (Nuopponen

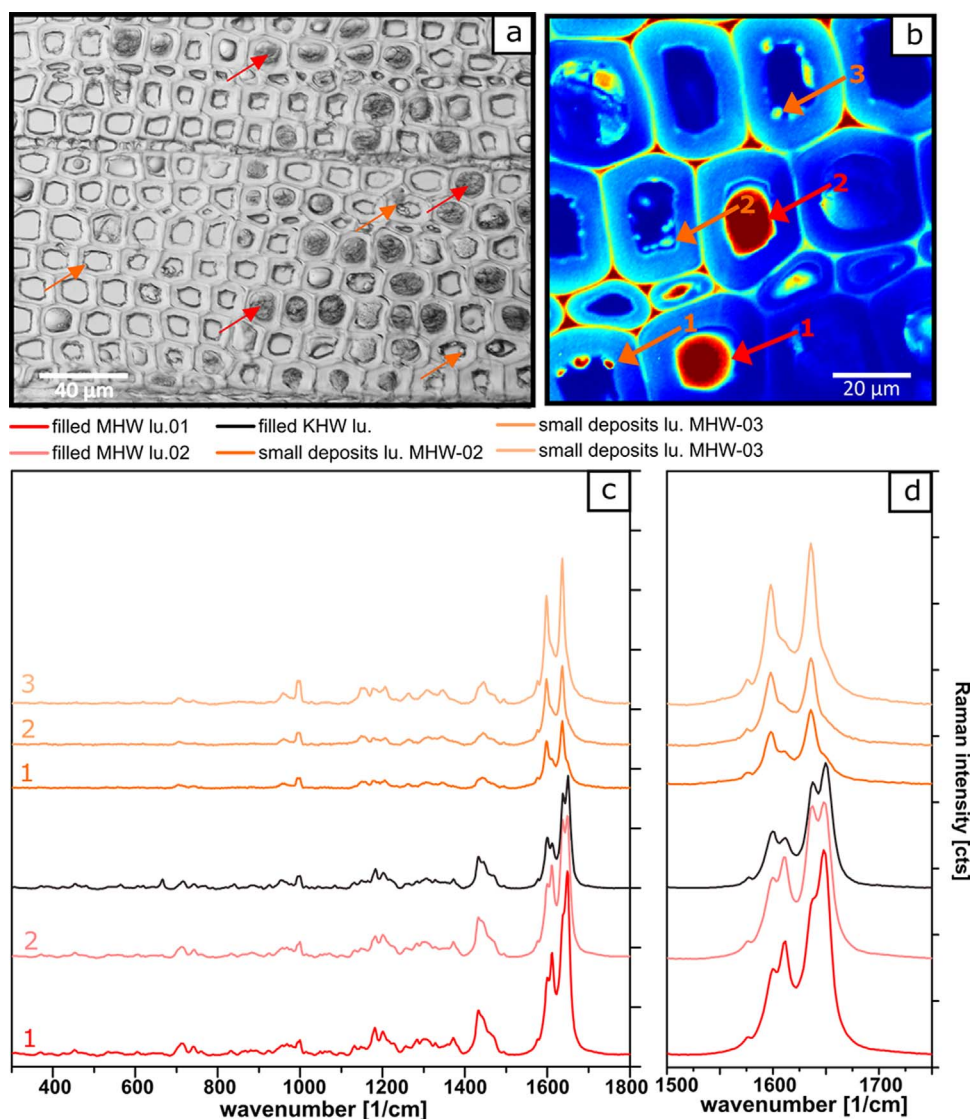


Fig. 5. Extractives deposits in middle heartwood (MHW). Light microscopy (a) and Raman (integration over the $1550\text{--}1700\text{ cm}^{-1}$) (b) images of unextracted IHW, showing the presence of filled lumens (red arrows) and small deposits (orange arrows), and Raman spectra of filled lumens and small deposits (c and d). (For interpretation of the references to colour in this figure legend, the reader is referred to the web version of this article.)

et al., 2004a). The resin acids probably originated from resin canals after the death of the epithelial cells, flowing into the lumens of tracheids whose pits were not blocked by aspiration or extractives incrustations (Hillis, 1987). As no resin acids could be detected in the CW or CC, it is possible that they occurred exclusively within cell lumina where they serve to further reduce the permeability of HW and KHW.

3.5. Analysis of ray cell contents

Heartwood extractives such as pinosylvins are formed in parenchyma cells, such as those that constitute the wood rays. Thus, the rays of HW and KHW were also analyzed for the presence of extractives. Raman images of MHW and KHW rays (Fig. 6a,b), obtained by integration of the combined lignin and extractives spectral region ($1550\text{--}1700\text{ cm}^{-1}$), showed the presence of large amounts of extractives within the rays. The distribution of extractives was uneven in both the MHW and KHW rays, and detailed analysis of the Raman spectra (Fig. 6c,d) revealed local differences in composition. The spectra of both MHW and KHW possessed bands at 995 , 1597 , and 1634 cm^{-1} , confirming that pinosylvins were present within the rays. However, an additional band at 1649 cm^{-1} showed that resin acids were also present. The presence of resin acids in the rays is not surprising, considering that many Scots pine rays contain embedded resin

canals. Due to their connection to the resin canal network, the rays are likely to be a means of distribution for the resin acids, which are known to be formed in the SW (Lim et al., 2016) but accumulate in large quantities in the HW and KHW.

4. Conclusions

In this work, the cellular level distributions of Scots pine HW and KHW extractives were studied by confocal Raman spectroscopy imaging. Pinosylvins were found in the CW, CC/CML, and lumina of tracheids, and their distribution suggested that their deposition into the cell walls can proceed via the CML or the lumen. Similarities were seen in the distribution of pinosylvins and lignin, pointing towards an interaction between the two components. The potential interaction of pinosylvins with lignin, in combination with their relatively low concentration in HW cell walls, could explain why the average decay resistance of Scots pine HW is only moderate. In contrast to the pinosylvins, resin acids were only detected within tracheid and ray cell lumina. In addition to understanding the properties of HW and the origins of natural durability, knowledge of the distribution of extractives will also prove valuable in wood preservation, modification, and functionalization activities, which often rely on the impregnation of wood cell walls with reactive molecules.

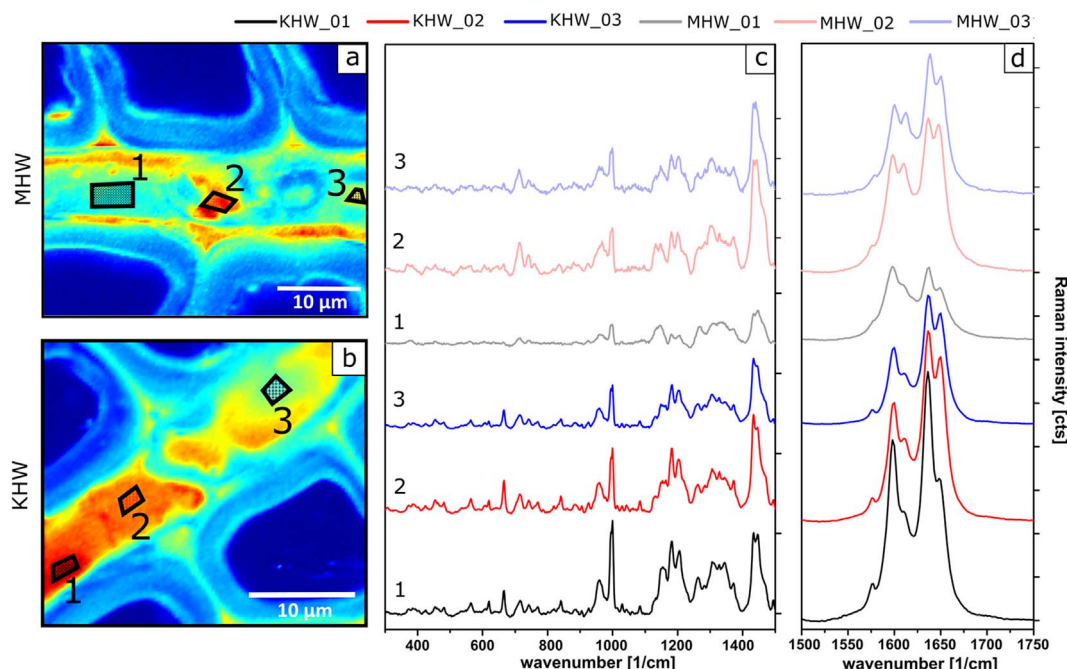


Fig. 6. Extractives within middle heartwood (MHW) and knot heartwood (KHW) rays. Raman imaging (integration over $1550\text{--}1700\text{ cm}^{-1}$) of IHW (a) and KHW (b) rays, showing measurement locations of spectra, and the Raman spectra of ray contents (c and d). (For interpretation of the references to colour in this figure legend, the reader is referred to the web version of this article.)

Acknowledgements

The authors would like to acknowledge support from COST Action FP1303 for STSM.

References

- Agarwal, U.P., Ralph, S.A., 2008. Determination of ethylenic residues in wood and TMP of spruce by FT-Raman spectroscopy. *Holzforschung* 62 (6), 667–675. <http://dx.doi.org/10.1515/hf.2008.112>.
- Agarwal, U.P., 2006. Raman imaging to investigate ultrastructure and composition of plant cell walls: distribution of lignin and cellulose in black spruce wood (*Picea mariana*). *Planta* 224 (5), 1141–1153. <http://dx.doi.org/10.1007/s00425-006-0295-z>.
- Arshadi, M., Backlund, I., Geladi, P., Bergsten, U., 2013. Comparison of fatty and resin acid composition in boreal lodgepole pine and Scots pine for biorefinery applications. *Ind. Crops Prod.* 49, 535–541. <http://dx.doi.org/10.1016/j.indcrop.2013.05.038>.
- Bergström, B., Gustafsson, G., Gref, R., Ericsson, A., 1999. Seasonal changes of pinosylvin distribution in the sapwood/heartwood boundary of *Pinus sylvestris*. *Trees Struct. Funct.* 14 (2), 65–71. <http://dx.doi.org/10.1007/pl00009754>.
- Bergström, B., 2003. Chemical and structural changes during heartwood formation in *Pinus sylvestris*. *Forestry* 76 (1), 45–53. <http://dx.doi.org/10.1093/forestry/76.1.45>.
- Billes, F., Mohammed-Ziegler, I., Mikosch, H., Holmgren, A., 2002. Vibrational spectroscopic and conformational analysis of pinosylvin. *J. Phys. Chem. A* 106 (26), 6232–6241. <http://dx.doi.org/10.1021/jp013218w>.
- Celimene, C.C., Micales, J.A., Ferge, L., Young, R.A., 1999. Efficacy of pinosylvin against white-rot and brown-rot fungi. *Holzforschung* 53 (5), 491–497. <http://dx.doi.org/10.1515/hf.1999.081>.
- Czamara, K., Majzner, K., Pacia, M.Z., Kochan, K., Kaczor, A., Baranska, M., 2015. Raman spectroscopy of lipids: a review. *J. Raman Spectrosc.* 46 (1), 4–20. <http://dx.doi.org/10.1002/jrs.4607>.
- Edwards, H.G.M., Farwell, D.W., Williams, A.C., 1994. FT-Raman spectrum of cotton – a polymeric biomolecular analysis. *Spectrochim. Acta Part A-Mol. Biomol. Spectrosc.* 50 (4), 807–811. [http://dx.doi.org/10.1016/0584-8539\(94\)80016-2](http://dx.doi.org/10.1016/0584-8539(94)80016-2).
- Ekeberg, D., Flåte, P.O., Eikenes, M., Fongen, M., Naess-Andresen, C.F., 2006. Qualitative and quantitative determination of extractives in heartwood of Scots pine (*Pinus sylvestris* L.) by gas chromatography. *J. Chromatogr. A* 1109 (2), 267–272. <http://dx.doi.org/10.1016/j.chroma.2006.01.027>.
- Ermeydan, M.A., Cabane, E., Masic, A., Koetz, J., Burgert, I., 2012. Flavonoid insertion into cell walls improves wood properties. *ACS Appl. Mater. Interfaces* 4 (11), 5782–5789. <http://dx.doi.org/10.1021/am301266k>.
- Fang, W.W., Hemming, J., Reunanen, M., Eklund, P., Pineiro, E.C., Poljanšek, I., Oven, P., Willför, S., 2013. Evaluation of selective extraction methods for recovery of polyphenols from pine. *Holzforschung* 67 (8), 843–851. <http://dx.doi.org/10.1515/hf-2013-0002>.
- Fengel, D., 1970. Ultrastructural changes during aging of wood cells. *Wood Sci. Technol.* 4 (3), 176–188.
- Fries, A., Ericsson, T., Gref, R., 2000. High heritability of wood extractives in *Pinus sylvestris* progeny tests. *Can. J. For. Res.* 30 (11), 1707–1713. <http://dx.doi.org/10.1139/cjfr-30-11-1707>.
- Gierlinger, N., Schwanninger, M., 2006. Chemical imaging of poplar wood cell walls by confocal Raman microscopy. *Plant Physiol.* 140 (4), 1246–1254. <http://dx.doi.org/10.1104/pp.105.066993>.
- Gierlinger, N., Luss, S., König, C., Konnerth, J., Eder, M., Fratzl, P., 2010. Cellulose microfibril orientation of *Picea abies* and its variability at the micron-level determined by Raman imaging. *J. Exp. Bot.* 61 (2), 587–595. <http://dx.doi.org/10.1093/jxb/erp325>.
- Gierlinger, N., Keplinger, T., Harrington, M., 2012. Imaging of plant cell walls by confocal Raman microscopy. *Nat. Protoc.* 7 (9), 1694–1708. <http://dx.doi.org/10.1038/nprot.2012.092>.
- Gierlinger, N., 2014. Revealing changes in molecular composition of plant cell walls on the micron-level by Raman mapping and vertex component analysis (VCA). *Front. Plant Sci.* 5. <http://dx.doi.org/10.3389/fpls.2014.00306>.
- Hänninen, T., Kontturi, E., Vuorinen, T., 2011. Distribution of lignin and its coniferyl alcohol and coniferyl aldehyde groups in *Picea abies* and *Pinus sylvestris* as observed by Raman imaging. *Phytochemistry* 72 (14–15), 1889–1895. <http://dx.doi.org/10.1016/j.phytochem.2011.05.005>.
- Harju, A.M., Venäläinen, M., 2002. Genetic parameters regarding the resistance of *Pinus sylvestris* heartwood to decay caused by *Coniophora puteana*. *Scand. J. For. Res.* 17 (3), 199–205. <http://dx.doi.org/10.1080/028275802753742864>.
- Harju, A.M., Kainulainen, P., Venäläinen, M., Tiitta, M., Viitanen, H., 2002. Differences in resin acid concentration between brown-rot resistant and susceptible Scots pine heartwood. *Holzforschung* 56 (5), 479–486. <http://dx.doi.org/10.1515/hf.2002.074>.
- Hart, J.H., Shrimpton, D.M., 1979. Role of stilbenes in resistance of wood to decay. *Phytopathology* 69 (10), 1138–1143. <http://dx.doi.org/10.1094/Phyto-69-1138>.
- Helm, R.F., Ranatunga, T.D., Chandra, M., 1997. Lignin-hydrolyzable tannin interactions in wood. *J. Agric. Food Chem.* 45 (8), 3100–3106. <http://dx.doi.org/10.1021/jf970083b>.
- Hillis, W.E., 1987. *Heartwood and Tree Exudates*. Springer-Verlag, Berlin.
- Holmgren, A., Bergström, B., Gref, R., Ericsson, A., 1999. Detection of pinosylvin in solid wood of Scots pine using Fourier transform Raman and infrared spectroscopy. *J. Wood Chem. Technol.* 19 (1–2), 139–150. <http://dx.doi.org/10.1080/02773819909349604>.
- Hovelstad, H., Leirset, I., Oyaas, K., Fiksdahl, A., 2006. Screening analyses of pinosylvin stilbenes, resin acids and lignans in Norwegian conifers. *Molecules* 11 (1), 103–114. <http://dx.doi.org/10.3390/11010103>.
- Imai, T., Tanabe, K., Kato, T., Fukushima, K., 2005. Localization of ferruginol, a diterpene phenol, in *Cryptomeria japonica* heartwood by time-of-flight secondary ion mass spectrometry. *Planta* 221 (4), 549–556. <http://dx.doi.org/10.1007/s00425-004-1476-2>.
- Jebrane, M., Pockrandt, M., Terziev, N., 2014. Natural durability of selected larch and Scots pine heartwoods in laboratory and field tests. *Int. Biodeterior. Biodegrad.* 91, 88–96. <http://dx.doi.org/10.1016/j.ibiod.2014.03.018>.
- Ji, Z., Ma, J.F., Zhang, Z.H., Xu, F., Sun, R.C., 2013. Distribution of lignin and cellulose in compression wood tracheids of *Pinus yunnanensis* determined by fluorescence microscopy and confocal Raman microscopy. *Ind. Crops Prod.* 47, 212–217. <http://dx.doi.org/10.1016/j.indcrop.2013.03.006>.

- Kampe, A., Magel, E., 2013. New insights into heartwood and heartwood formation. In: Fromm, J. (Ed.), *Cellular Aspects of Wood Formation*. Springer, Berlin, pp. 71–95.
- Karppanen, O., Venäläinen, M., Harju, A.M., Willför, S., Pietarinen, S., Laakso, T., Kainulainen, P., 2007. Knotwood as a window to the indirect measurement of the decay resistance of Scots pine heartwood. *Holzforschung* 61 (5), 600–604. <http://dx.doi.org/10.1515/hf2007.091>.
- Keplinger, T., Cabane, E., Chanana, M., Hass, P., Merk, V., Gierlinger, N., Burgert, I., 2015. A versatile strategy for grafting polymers to wood cell walls. *Acta Biomater.* 11, 256–263. <http://dx.doi.org/10.1016/j.actbio.2014.09.016>.
- Kuo, M.-L., Arganbright, D.G., 1980. Cellular distribution of extractives in Redwood and Incense Cedar – part II: microscopic observation of the location of cell wall and cell cavity extractives. *Holzforschung* 34 (2), 41–47.
- Leinonen, A., Harju, A.M., Venäläinen, M., Saranpää, P., Laakso, T., 2008. FT-NIR spectroscopy in predicting the decay resistance related characteristics of solid Scots pine (*Pinus sylvestris* L.) heartwood. *Holzforschung* 62 (3), 284–288. <http://dx.doi.org/10.1515/hf.2008.033>.
- Lim, K.J., Paasela, T., Harju, A., Venäläinen, M., Paulin, L., Auvinen, P., Kärkkäinen, K., Teeri, T.H., 2016. Developmental changes in Scots pine transcriptome during heartwood formation. *Plant Physiol.* 172 (3), 1403–1417. <http://dx.doi.org/10.1104/pp.16.01082>.
- Lu, J.R., Venäläinen, M., Julkunen-Tiitto, R., Harju, A.M., 2016. Stilbene impregnation retards brown-rot decay of Scots pine sapwood. *Holzforschung* 70 (3), 261–266. <http://dx.doi.org/10.1515/hf-2014-0251>.
- Merk, V., Chanana, M., Keplinger, T., Gaan, S., Burgert, I., 2015. Hybrid wood materials with improved fire retardance by bio-inspired mineralisation on the nano- and sub-micron level. *Green Chem.* 17 (3), 1423–1428. <http://dx.doi.org/10.1039/c4gc01862a>.
- Mohammed-Ziegler, I., Holmgren, A., Forsling, W., Lindberg, M., Ranheimer, M., 2004. Mechanism of the adsorption process of pinosylvin and some polyhydroxybenzenes onto the structure of lignin. *Vib. Spectrosc.* 36 (1), 65–72. <http://dx.doi.org/10.1016/j.vibspec.2004.03.001>.
- Nagasaki, T., Yasuda, S., Imai, T., 2002. Immunohistochemical localization of agatharesinol, a heartwood norlignan, in *Cryptomeria japonica*. *Phytochemistry* 60 (5), 461–466. [http://dx.doi.org/10.1016/S0031-9422\(02\)00141-3](http://dx.doi.org/10.1016/S0031-9422(02)00141-3).
- Nuopponen, M., Willför, S., Jääskeläinen, A.S., Sundberg, A., Vuorinen, T., 2004a. A UV resonance Raman (UVR) spectroscopic study on the extractable compounds of Scots pine (*Pinus sylvestris*) wood part I: Lipophilic compounds. *Spectrochim. Acta Part A-Mol. Biomol. Spectrosc.* 60 (13), 2953–2961. <http://dx.doi.org/10.1016/j.saa.2004.02.008>.
- Nuopponen, M., Willför, S., Jääskeläinen, A.S., Vuorinen, T., 2004b. A UV resonance Raman (UVR) spectroscopic study on the extractable compounds in Scots pine (*Pinus sylvestris*) wood – part II. Hydrophilic compounds. *Spectrochim. Acta Part A-Mol. Biomol. Spectrosc.* 60 (13), 2963–2968. <http://dx.doi.org/10.1016/j.saa.2004.02.007>.
- Piispanen, R., Saranpää, P., 2002. Neutral lipids and phospholipids in Scots pine (*Pinus sylvestris*) sapwood and heartwood. *Tree Physiol.* 22 (9), 661–666.
- Plaschkies, K., Jacobs, K., Scheiding, W., Melcher, E., 2014. Investigations on natural durability of important European wood species against wood decay fungi. Part 1: laboratory tests. *Int. Biodeterior. Biodegrad.* 90, 52–56. <http://dx.doi.org/10.1016/j.ibiod.2014.01.016>.
- Streit, W., Fengel, D., 1994. Heartwood formation in Quebracho colorado (*Schinopsis balansae* engl) – tannin distribution and penetration of extractives into the cell walls. *Holzforschung* 48 (5), 361–367. <http://dx.doi.org/10.1515/hfsg.1994.48.5.361>.
- Talian, I., Orinak, A., Efremov, E.V., Ariese, F., Kaniansky, D., Orinakova, R., Hubner, J., 2010. Detection of biologically active diterpenic acids by Raman Spectroscopy. *J. Raman Spectrosc.* 41 (9), 964–968. <http://dx.doi.org/10.1002/jrs.2545>.
- Taylor, A.M., Gartner, B.L., Morrell, J.J., 2002. Heartwood formation and natural durability – a review. *Wood Fiber Sci.* 34 (4), 587–611.
- Venäläinen, M., Harju, A.M., Saranpää, P., Kainulainen, P., Tiitta, M., Velling, P., 2004. The concentration of phenolics in brown-rot decay resistant and susceptible Scots pine heartwood. *Wood Sci. Technol.* 38 (2), 109–118. <http://dx.doi.org/10.1007/s00226-004-0226-8>.
- Willför, S., Hemming, J., Reunanen, M., Holmbom, B., 2003. Phenolic and lipophilic extractives in Scots pine knots and stemwood. *Holzforschung* 57 (4), 359–372. <http://dx.doi.org/10.1515/hf.2003.054>.
- Willför, S., Reunanen, M., Eklund, P., Sjöholm, R., Kronberg, L., Fardim, P., Pietarinen, S., Holmbom, B., 2004. Oligolignans in Norway spruce and Scots pine knots and Norway spruce stemwood. *Holzforschung* 58 (4), 345–354. <http://dx.doi.org/10.1515/hf.2004.053>.
- Zhang, C.H., Fujita, M., Takabe, K., 2004. Extracellular diffusion pathway for heartwood substances in *Albizia julibrissin* Durazz. *Holzforschung* 58 (5), 495–500. <http://dx.doi.org/10.1515/hf.2004.075>.
- Zhou, X., Ma, J., Ji, Z., Zhang, X., Ramaswamy, S., Xu, F., Sun, R.C., 2014. Dilute acid pretreatment differentially affects the compositional and architectural features of *Pinus bungeana* Zucc. compression and opposite wood tracheid walls. *Ind. Crops Prod.* 62, 196–203. <http://dx.doi.org/10.1016/j.indcrop.2014.08.035>.